Metadata of the chapter that will be visualized in SpringerLink

Book Title	TMS 2022 151st Annual Meeting & Exhibition Supplemental Proceedings	
Series Title		
Chapter Title	In Situ Observation of Coupled Growth Morphologies in Organic Peritectics Under Pure Diffusion Conditions	
Copyright Year	2022	
Copyright HolderName	The Minerals, Metals & Materials Society	
Corresponding Author	Family Name	**Mogeritsch**
	Particle	
	Given Name	**Johann**
	Prefix	
	Suffix	
	Role	
	Division	Department Metallurgy
	Organization	University of Leoben
	Address	Franz-Josef-Strasse 18, 8700, Leoben, Austria
	Email	johann.mogeritsch@unileoben.ac.at
Author	Family Name	**Sillekens**
	Particle	
	Given Name	**Wim**
	Prefix	
	Suffix	
	Role	
	Division	
	Organization	European Space Agency ESA, ESTEC
	Address	Keplerlaan 1, 2201 AZ, Noordwijk, Netherlands
	Email	
Author	Family Name	**Ludwig**
	Particle	
	Given Name	**Andreas**
	Prefix	
	Suffix	
	Role	
	Division	Department Metallurgy
	Organization	University of Leoben
	Address	Franz-Josef-Strasse 18, 8700, Leoben, Austria
	Email	

Abstract	Isothermally coupled peritectic solidification for a hyper-peritectic alloy under pure diffusive conditions is presented. For this purpose, directional solidification experiments were performed aboard the International Space Station using a model system for peritectic layer solidification patterns. At constant temperature gradient of 3.0 K/mm and for pulling velocities ranging from 0.12 µm/s to 0.09 µm/s, coupled peritectic growth was observed. At lower pulling velocities, contrary to expectations, only a planar solidification

front of the pro-peritectic phase was detected. Two effects were noticed: a significant effect of the pro-peritectic interface on the capability of the peritectic phase to nucleate and, in the further course of the experiments, a dynamic change of the coupled peritectic growth microstructure.

Keywords (separated by '-')	Peritectic solidification - International space station - Microgravity - TRIS-NPG

In Situ Observation of Coupled Growth Morphologies in Organic Peritectics Under Pure Diffusion Conditions

Johann Mogeritsch, Wim Sillekens, and Andreas Ludwig

Abstract Isothermally coupled peritectic solidification for a hyper-peritectic alloy under pure diffusive conditions is presented. For this purpose, directional solidification experiments were performed aboard the International Space Station using a model system for peritectic layer solidification patterns. At constant temperature gradient of 3.0 K/mm and for pulling velocities ranging from 0.12 μm/s to 0.09 μm/s, coupled peritectic growth was observed. At lower pulling velocities, contrary to expectations, only a planar solidification front of the pro-peritectic phase was detected. Two effects were noticed: a significant effect of the pro-peritectic interface on the capability of the peritectic phase to nucleate and, in the further course of the experiments, a dynamic change of the coupled peritectic growth microstructure.

Keywords Peritectic solidification · International space station · Microgravity · TRIS-NPG

Introduction

A peritectic reaction is the solidification of a liquid L and the transformation of an already existing primary solid phase α into a second solid peritectic phase β ($L + \alpha \rightarrow \beta$) at the invariant peritectic temperature T_P. The interesting characteristic in peritectic systems is the possibility of forming peritectic phase β above the peritectic temperature. From a thermodynamic point of view, an alloy with a concentration C_0 within the peritectic plateau $C_\alpha \leq C_0 \leq C_l$ should start to solidify with the primary pro-peritectic α phase which transforms to the peritectic β phase when the interface temperature goes below the peritectic temperature. Under conditions where the solidification morphology for one or both phases is planar, it was found

J. Mogeritsch (✉) · A. Ludwig
Department Metallurgy, University of Leoben, Franz-Josef-Strasse 18, 8700 Leoben, Austria
e-mail: johann.mogeritsch@unileoben.ac.at

W. Sillekens
European Space Agency ESA, ESTEC, Keplerlaan 1, 2201 AZ Noordwijk, Netherlands

The Minerals, Metals & Materials Society (ed.), *TMS 2022 151st Annual Meeting & Exhibition Supplemental Proceedings*, The Minerals, Metals & Materials Series, https://doi.org/10.1007/978-3-030-92381-5_136

523312_1_En_136_Chapter ☑ TYPESET ☐ DISK ☐ LE ☑ CP Disp.:30/11/2021 Pages: 13 Layout: T1-Standard

that within the peritectic plateau two microstructures occur: (i) oscillations of the concentration in liquid close by the solid/liquid (s/l) interface forming an alternating growth sequence in form of bands of both phases parallel to the solidification front, or (ii) simultaneous growth of both phases in the form of fibers or lamellae, called peritectic coupled growth (PCG), similar to a regular eutectic growth front, whereby peritectic layer structures are highly sensitive to convection ahead of the solidification front.

In fact, depending on the material properties and the intensity of convection, peritectic alloys showed in directional solidification experiments a variety of complex microstructures like isothermal peritectic coupled growth (IPCG), cellular peritectic coupled growth, discrete bands, island bands, or oscillatory tree-like structures [1–6].

To explain the experimentally obtained microstructures, several models were published. Trivedi [7] issued a model which explains cyclic nucleation and overgrowth under purely diffusive growth conditions in the hypo-peritectic region ($C_\alpha \leq C_0 \leq C_p$). The theory predicts that the pro-peritectic and peritectic phases would grow independently and alternately as planar fronts below (pro-peritectic phase) and above (peritectic phase) the peritectic temperature. Since the model cannot explain the huge variation of experimentally obtained peritectic solidification patterns, and convection is nearly always present on Earth, advanced models were published. Hunzinger's model [8] was based on the nucleation and constitutional undercooling criterion under the assumption of infinitely high nuclei density and steady-state growth and Lo et al. [9] showed by simulation that bands are formed only for approximately equal volume fraction of the two phases; otherwise, islands bands are formed. Trivedi [10] revised and updated his theory as related to the role of heterogeneous nucleation on the microstructure evolution.

The authors analyzed layered peritectic structures by using an organic model system instead of metallic alloys. Organic components with a high-temperature transparent non-faceted phase, called plastic phase, solidify metal-like. The transparency of the phases enables the real-time observation of the solidification dynamics with a light microscope. The binary peritectic system TRIS–NPG [11] was selected for directional solidification experiments with compositions within the peritectic plateau. The studies confirmed the peritectic microstructures found in metal alloys, but also provided insight into the dynamics leading to peritectic layered structures [12–15] as mentioned above. It was also found that in the case where both phases grew separately the competing growth resulted in alternating oscillating interfaces of the two phases [15].

In this article, we describe the experimental findings for directional solidification experiments under purely diffusive conditions. For this, a hyper-peritectic concentration was processed aboard the International Space Station (ISS).

523312_1_En_136_Chapter ☑ TYPESET ☐ DISK ☐ LE ☑ CP Disp.:30/11/2021 Pages: 13 Layout: T1-Standard

Experimental Procedure

In this section, we describe (i) the equipment used aboard the ISS, (ii) the alloy preparation, and (iii) the selected process conditions.

(1) The directional solidification experiments were carried out aboard the ISS. For this purpose, the TRANSPARENT ALLOYS (TA) instrument was used. This device was specially developed by the European Space Agency (ESA) and QinetiQ Space for microgravity (μg) experiments with organic transparent alloys and was installed in the Microgravity Science Glovebox (MSG). The main part of the TA experiment unit is the Bridgman assembly, a thermal unit with two hot clamps, called hot zone, on one side, and two cold clamps, called cold zone, on the other side, as shown in Fig. 1. The Bridgman furnace had a distinct temperature gradient created by the hot and cold clamps temperature. The hot clamps had temperatures higher than the melting point, and the cold clamps had temperatures lower than the melting point. A 7 mm width gap between the hot and cold clamps acts as an adiabatic zone.

A glass cartridge filled with the organic alloy and set in between the clamps was slowly pulled from the hot zone into the cold zone (cartridge travel), whereby the organic material in the cartridge was completely molten in the hot zone and the s/l interface was positioned within the adiabatic gap.

The special designed Transparent Alloy Cartridge (TAC) consisted of a quartz window clamped in between 2 stainless steel parts. The TAC had a solidification volume of 100 mm (length) × 6 mm (width) × 1 mm (depth).

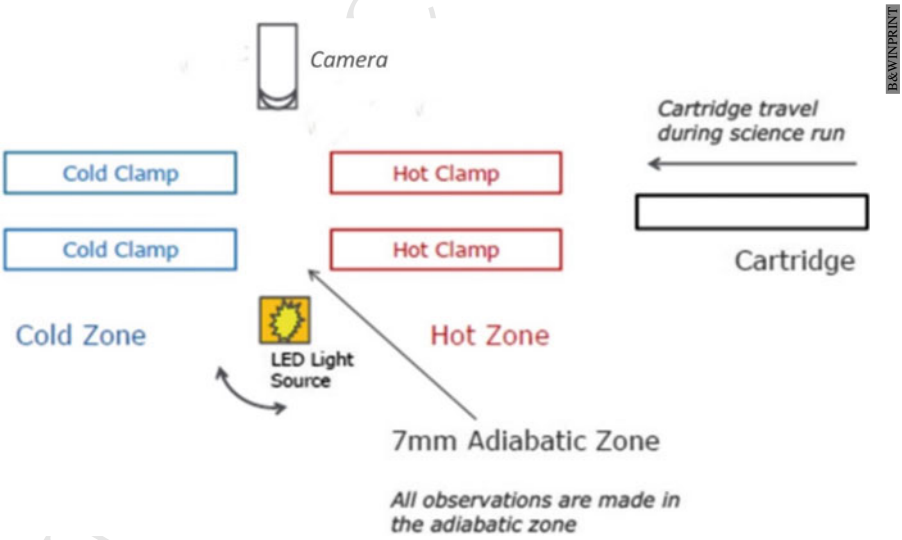

Fig. 1 Sketch of the Bridgman furnace assembly within transparent alloys device. *Source* QinetiQ Space, Kruibeke, Belgium [16]

Due to the necessary minimum contact areas with the hot and cold clamps, an effective solidification length of 66 mm was available.

The optical set-up includes an LED light source illumination system and a CCD camera centered on the adiabatic zone with a Field of View (FOV) of 6.1×5.1 mm^2. During the experiments, a set of 3 images were taken with a time step of 3 s at 3 different focal depths, $foc_1 = 0$ mm, directly on the inside of the front glass wall, $foc_2 = 0.5$ mm, in the middle of the cartridge, and $foc_3 = 0.8$ mm, close to the rear glass wall. A set of new images were shot each 30 s. The execution of the tests on board was supervised by the authors. For this purpose, only one single image set was transmitted from the ISS to the authors every hour. The findings presented in this paper are based on these images.

(ii) The organic component TRIS (tris(hydroxymethyl)aminomethane) was employed in combination with the organic component NPG (Neopentylglycol) as a model system for metal-like peritectic solidification under µg-conditions aboard the ISS. Both organic substances have at low temperature faceted phases and at high-temperature transparent orientationally disordered crystals (short form ODIC), usually called plastic crystal, which forms in an intermediate concentration range a peritectic equilibrium. It should be noted that there are several publications of the TRIS-NPG phase diagram. These are based either on experimental investigations or on thermodynamic calculations, showing an enlarged concentration range with respect to the peritectic plateau. The phase diagram [11] used by the authors to define the process conditions is based on experimental data. Details on the peritectic plateau and the used alloy concentration at $x = 0.53$ mol fraction NPG are shown in Fig. 2.

TRIS and NPG were delivered as powder from Sigma Aldrich [17] with an indicated purity of 99.9 + % and 99%, respectively. Both substances are highly hydroscopic [18], whereby the water content of the organic substance NPG was reduced by a drying process at 375 K for 24 h. TRIS, sensitive to long time annealing at temperatures above the faceted transformation temperature, and delivered with high-purity, was used without further purification. The alloy manufacturing was performed by the authors, while the TAC filling was done by QinetiQ Space and their on-orbit processing operated from ground by E-USOC under the coordination of the ESA.

(iii) Peritectic layered structures are expected for process conditions where both phases grow planar that occurs at solidification rates below the critical velocity [19]. For this purpose, a temperature gradient of 3.0 K/mm was set in the adiabatic zone and the TAC was drawn with a pulling velocity V_p from the hot zone to the cold zone in discrete steps of 0.01 µm in the range of $0.08 \leq V_p \leq 0.12$ µm/s.

The 66 mm observable part of the cartridge was virtual evenly divided into 6 starting points that created 6 equal lengths of 11 mm, called in this paper segments. This allowed 6 different solidification experiments to be performed with a fresh segment that has never been molten before. Due to the lack of convection in the melt under µg-conditions, segments that had been processed

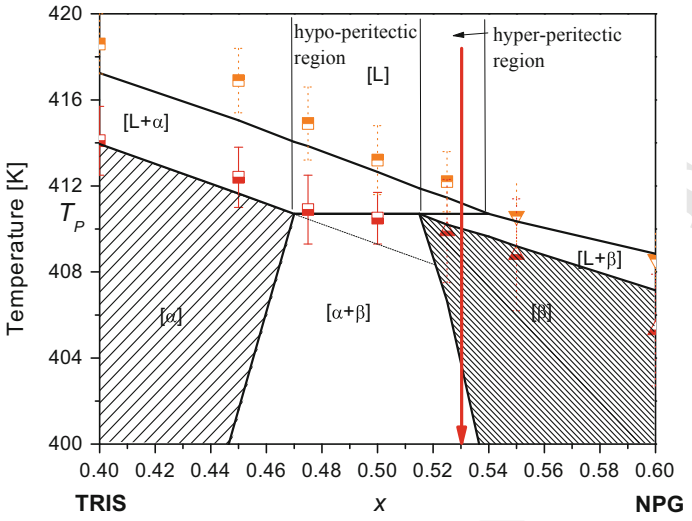

Fig. 2 Peritectic region of the system TRIS-NPG. The squares show the liquidus (black/white rectangles) temperature, the solidus (white/black rectangles) temperature, and the peritectic temperature T_p for the TRIS-rich side published by [11]. The triangles show the corresponding situation for the NPG-rich side. The straight lines are placed by the authors to approach the published measured points. The dashed line shows the extension of the solidus line of the pro-peritectic phase into the metastable region

already and that are now located in the hot zone and are thus liquid do not interact with the new fresh segment. The experiments started with segment 1 that was at the beginning in the hot zone and were then continued in ascending order. This guaranteed that all the segments already processed were in the hot zone.

Each experiment consisted of the same sub-sequences. First, the temperature on all clamps was set on 440 K and the alloy within the TAC was annealed for 2 h. Afterwards, the temperature in the cold zone was set to 403 K and the temperature in the hot zone was set to 503 K. The TAC was kept in rest for one hour to perform thermal equilibrium within the device. Finally, the actually solidification experiment was activated and the TAC was processed between 8 and 30 h.

Results

The results presented in this paper are from the author's µg-experiments aboard the ISS, in particular, the solidification morphologies for a hyper-peritectic organic alloy with $x = 0.53$ mol fraction NPG under pure diffusion conditions. The results pointed out nucleation events that resulted in IPCG for pulling velocities in the range of

0.09 μm/s $\geq V_p \geq$ 0.11 μm/s. For $V_p = 0.12$ μm/s, a nucleation event was observed, but the initial planar s/l liquid interface transformed into a cellular/dendritic one. In contrast, for a pulling velocity of $V_p = 0.08$ μm/s, the initial planar pro-peritectic phase grew, but no nucleation event was detected.

Initially after thermal equilibration, the plastic phase showed a polycrystalline structure. It should be noted that according to the phase diagram, the polycrystalline plastic phase consisted of the pro-peritectic phase and the peritectic phase. Due to the identical optical properties of both phases, it was not possible to determine whether both phases were really present. When the sample was moved, the pro-peritectic phase started to grow until for the pulling velocities mentioned above the nucleation event occurred.

In this section, we describe, as examples, (i) the microstructure of a coupled peritectic growth and its main features, and (ii) we exhibit the dynamics of peritectic coupled growth for the pulling velocities mentioned above by presenting partial cuttings of the s/l interface.

(i) In Fig. 3, the main features of the transparent alloy during peritectic coupled growth for $V_p = 0.11$ μm/s after an experiment duration of 17 h are presented. The image was taken where the camera focus was set on $foc_1 = 0$ mm. Hence, all structures close to the inner side of the front glass wall showed sharp lines, whereas all others pattern exhibited a more or less a blurred form. The matrix phase grew planar while the peritectic phase solidified as fibers within the matrix. The fibers were 27 ± 7 μm diameter, and the distance between the rods was $\lambda = 230 \pm 40$ μm. The diameter of the fibers revealed a slightly

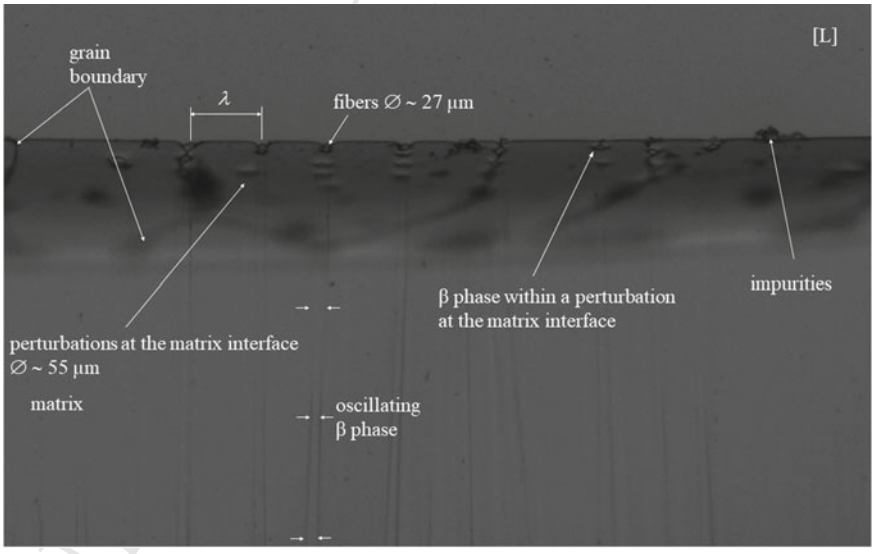

Fig. 3 Peritectic coupled growth of the hyper-peritectic alloy for a pulling velocity of $V_p =$ 0.11 μm/s. The β phase grows fibers-like within the α phase matrix (width of the image = 2.55 mm)

oscillating behavior within the plastic phase. It has to be mentioned that the s/l interface was wavy in such a way that the interface was inclined with the lowest position at the rear glass wall/material interface. This can be seen from the shadow effect in the plastic phase at the interface with the melt. A result due to slight temperature deviations in the control of the clamps. The effect proved useful in retrospect because it made the dynamics of growth more observable. Grain boundaries were recognized as curved lines close to and/or in contact with the s/l interface, as well as impurities in the melt which accumulated in front of the solidification front. The s/l interface showed few perturbations with a diameter of up to 55 µm. In some perturbations, the growth of the peritectic phase was visible. Since the pro-peritectic and the peritectic phases were transparent, the simultaneous growth of both phases was only recognizable by the formation of phase boundaries, exhibited as dark lines, within the plastic phases.

(ii) Figures 4, 5, 6 and 7 show the solidification pattern shortly after a nucleation event of the peritectic phase and the dynamics of coupled growth for four different pulling velocities, namely $V_p = 0.12$, 0.11, 0.10, and 0.09 µm/s. All experiments have in common that the peritectic patches failed to spread along

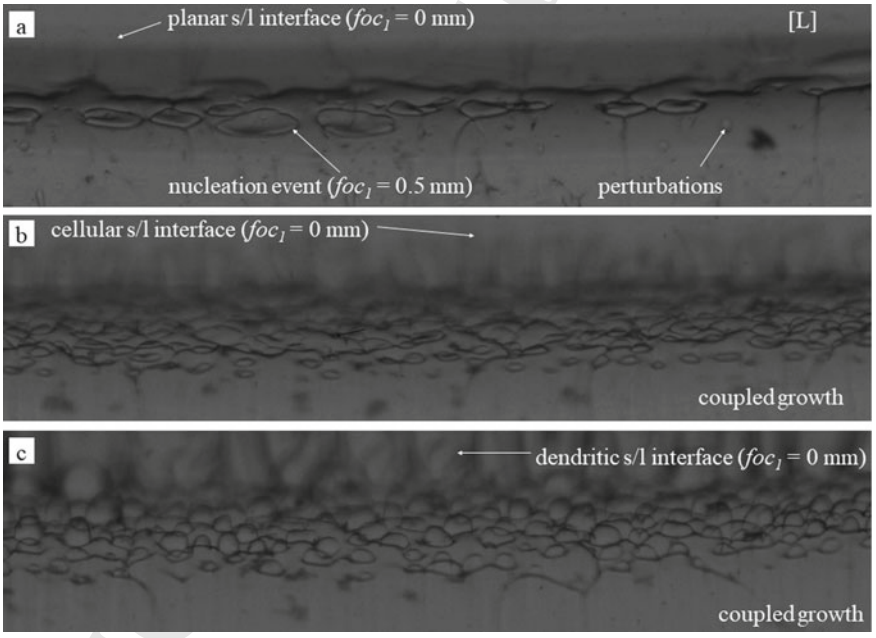

Fig. 4 Solidification pattern evolution after a nucleation event that happened at a pulling velocity of $V_p = 0.12$ µm/s within the TAC center ($foc_2 = 0.5$ mm). The initial s/l interface grew planar. The β phase grows fiber-like within the α matrix before bath phases grew in a cellular/dendritic manner (width of the image = 2.55 mm)

the α interface and grew together, a precondition for banded growth; instead, IPCG was formed.

The results for $V_p = 0.12$ μm/s are explained in Fig. 4. Figure 4a shows the solidification pattern shortly after a nucleation event has taken place with a focus setting $foc_2 = 0.5$ mm (TAC center). Few perturbations were visible at the s/l interface in the form of small rings. The peritectic phase can be recognized by the pancake-like structures. However, the β phase did not begin to spread out over the α phase to form a band. On the contrary, it can be seen that the number of local regions exhibiting β-phase increases but decreases in size, compare Fig. 4a, b. Additionally, fine blurry lines can be detected within the plastic phase. These blurry lines were the indication for solid–solid interfaces within the plastic phase occurring during coupled growth (Fig. 4b). After nucleation, the peritectic phase grew at the same temperature level as the α phase, or slightly below, whereas, in Fig. 4c, the interface of the peritectic phase grew at a higher temperature level as the surrounding pro-peritectic phase. This indicated the transition from a planar growth to a cellular/dendritic growth. In the upper part of each image (Fig. 4a–c), the s/l interface close to the glass wall can be detected as blurred line since it was not in focus. This blurry interface, which was still planar in Fig. 4a, formed already a cellular solidification structure in Fig. 4b and grew cellular/dendritic in Fig. 4c.

The peritectic coupled growth observed for $V_p = 0.11$ μm/s is shown in Fig. 5. Note that the images were brightened to lighten the pattern just after nucleation. As a result, the coupled growth is no longer clearly visible as in Fig. 3. Initially, the peritectic phase appeared in a pancake-like shape, as shown in Fig. 5a. It seems to be that the nucleation density was higher than in the previous experiment, see Figs. 4a and 5a. Initially, the β phase grew in a lamellar-like manner, recognizable by the zig-zag growth pattern at the

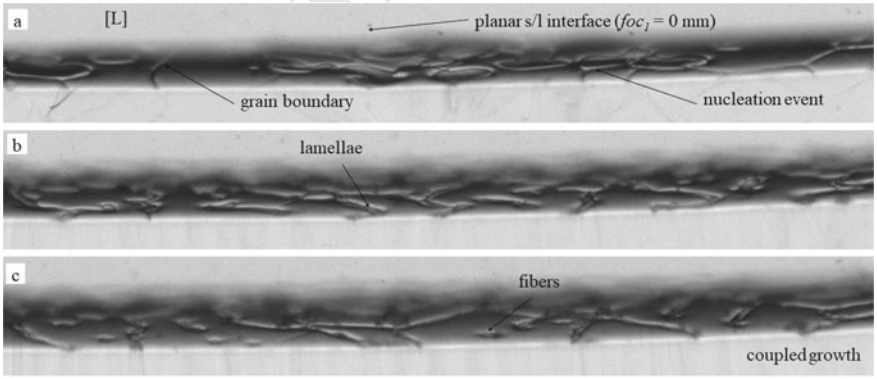

Fig. 5 Peritectic coupled growth of the hyper-peritectic alloy for a pulling velocity of $V_p = 0.11$ μm/s. **a** taken just after the nucleation event, **b** after a while the peritectic phase grew lamellae-like, and **c** later even fibers-like within the pro-peritectic phase (width of the image = 2.55 mm)

523312_1_En_136_Chapter ☑ TYPESET ☐ DISK ☐ LE ☑ CP Disp.:30/11/2021 Pages: 13 Layout: T1-Standard

s/l interface (Fig. 5c). This zig-zag pattern leads to an overlap of the phase boundaries in the plastic phase and thus prevented the evaluation of the lateral phase growth. As the experiment progressed, the proportion of the β phase decreased, evident by the transition from lamellar growth to a fibrous structure. After 10 h of coupled growth, the β phase disappeared and only the α phase grew planar.

The results for a pulling velocity of $V_p = 0.10$ µm/s were similar to the findings of the experiment described previously. The nucleation events were followed by lamellar growth which transformed into a fibers-like growth (Fig. 6a–c). Nonetheless, differences can be detected. The nucleation density and the proportion of the ß phase were higher as for $V_p = 0.11$ µm/s. The coupled growth could be observed for 18 h, when the experiment was aborted.

The findings for $V_p = 0.09$ µm/s were isothermal peritectic coupled growth after nucleation of the β phase. The nucleation density and phase fraction were lower than in the previously described experiments. In Fig. 7a, the peritectic phase nucleated at different positions at the s/l interface and spread out in a circle form. The peritectic coupled growth morphology shows, as described in the experiments before, first a lamellar growth structure which transforms in the further course of the solidification experiments into a fiber-like one (Fig. 7b, c). The proportion of the new phase decreased as the experiment progresses until only the planar growth of the α phase was observed. For pulling velocities $V_p \leq 0.08$ µm/s, no nucleation event was observed and only the initial existing phase grew.

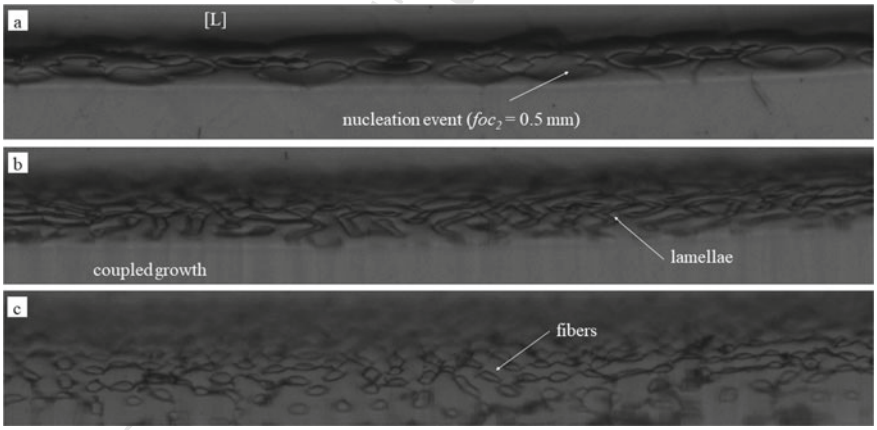

Fig. 6 Peritectic coupled growth of the hyper-peritectic alloy for a pulling velocity of $V_p = 0.10$ µm/s. **a** taken just after the nucleation event, **b** peritectic coupled growth that shows a lamellar zig-zag structure, and **c** transformation of the zig-zag structure into a fibers-like coupled growth (width of the image = 2.55 mm)

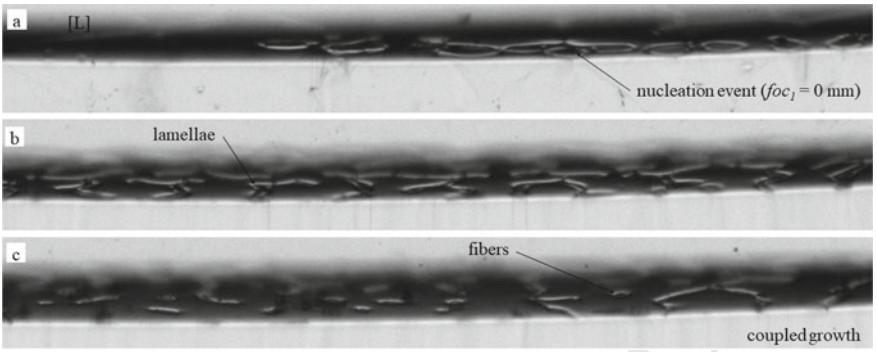

Fig. 7 Peritectic coupled growth of the hyper-peritectic alloy for a pulling velocity of V_p = 0.09 μm/s. **a** circular spreading of the peritectic phase after the nucleation event, **b** lamellar growth that transitions into **c** fibrous growth (width of the image = 2.55 mm)

Discussion

The results of μg solidification experiments for a hyper-peritectic alloy that showed a nucleation event are presented and details with respect to (i) the temperature range for the nucleation event, (ii) the temperature level of the s/l interface, and (iii) the change in microstructure during coupled growth are now discussed. For each subject, we compared the experimental results with Trivedi's models [7, 10].

(i) The onset of the nucleation events was observed at the s/l interface at a temperature of $T_{nuc} = 408.5 \pm 1.0$ K. That the nucleation event took place below the peritectic temperature agrees with expectations. Only when the concentration in the melt before the solidification front reaches the supercooling necessary for the formation of the peritectic phase (here determined to be $T_u = 2.2$ K), the β phase nucleates. However, it should be noted that the published temperature accuracy is in the order of ± 2 K.

After nucleation, the peritectic phase grew circular from several nucleation points. Since all nucleated regions showed a minor depression within the center, we assume that the peritectic phase nucleated in perturbations at the planar s/l interface of the α phase. Immediately after the first embryos were formed, the β phase grew radially along the interface between the melt and the α phase. This happened until the β phase almost filled the depression within the matrix, but did not exceed the temperature level of the α-liquid interface. It can be noted that the proportion of the peritectic phase increased when the pulling velocity was reduced. At a pulling velocity of $V_P = 0.10$ μm/s, the largest proportion of peritectic phase was observed. The peritectic phase fraction decreased by a further decrease of the pulling velocity. Finally, no nucleation event was observed for a pulling velocity of $V_p = 0.08$ μm/s. Thus, there seems to be a pulling velocity that creates the optimal wetting conditions for the peritectic phase to nucleate at the pro-peritectic matrix.

Trivedi predicted that the developing microstructure depends on nucleation and growth competition between the primary and peritectic phases. Single nucleation at the wall and subsequent spreading of the nucleating phase across the interface result in discrete bands or sub-bands. If nucleation occurs at the s/l interface, particulate bands or peritectic coupled growth can form. In the present case, the nucleation event was governed by the wetting conditions of the peritectic phase on depressions of the primary phase and the nucleation event at the s/l interface led to peritectic coupled growth. Thereby, the μg-experiments confirmed Trivedi's forecast.

(ii) Initially, the temperatures of the s/l interface were at the liquidus temperature. Once the TAC was moved from the hot zone to the cold zone, the s/l interface attempted to compensate this movement by planar growth. Simultaneously, an NPG-enriched boundary layer forms in front of the interface and the temperature level of the s/l interface decreases continuously. In theory, the nucleation of the peritectic phase is possible as soon as the NPG-enriched liquid interface layer dropped below the peritectic temperature. In the absence of any nucleation events, a steady state for planar growth will be reached at the solidus temperature of the pro-peritectic phase. It should be noted that at no time and in all experiments, the growth rate of the organic alloy was sufficient to a reach steady-state condition.

Here, nucleation occurred below the peritectic temperature and above the solidus temperature. The solidus temperature was determined by the authors by a simple linear extension in the metastable region. In the further course of the experiment, the solidification front did not grow at a constant temperature as expected. Instead, the s/l interface temperature level continuously decreased and was finally below the presumed α solidus temperature. This is in contrast to the fact that the peritectic temperature in a binary diagram is an invariant temperature. Nonetheless, it is true that at the s/l interface the melt and both solid phases were in equilibrium ($L \rightarrow \alpha + \beta$) and that at a constant decreasing temperature level. If the growth of both phases is considered separately from each other, then both phases would try to grow planar at their own solidus line. If both solidus temperatures are in lower temperature ranges, the coupled growth and the simultaneous reduction of the s/l interface temperature could be explained. However, this is a speculative assumption and an answer to this question must be postponed pending further investigation.

(iii) Regarding the shape of the peritectic phase at the s/l interface, lamellar-like structures formed after the nucleation process. In the further course of the solidification experiments, the lamellae became smaller and transformed into fiber-like structures. This indicates that the amount of peritectic phase was not constant and the fraction of growing peritectic phase decreased as well as the temperature level at the s/l interface. When the interfacial temperature fell below 401 ± 2 K, the peritectic phase, and thus the coupled growth, disappeared. It should be noted that this corresponds to the range of temperature at which, according to the phase diagram (Fig. 2), the concentration line intersects the phase boundary $\alpha + \beta/\beta$.

Summary and Conclusions

Directional solidification experiments were performed under μg-conditions aboard the ISS. The experimental findings presented above can be summarized as follows:

- Trivedi predicted peritectic layered structures under pure diffusion conditions. He forecasts that depending on the nucleation conditions band or coupled growth formed. Our directional solidification experiments showed nucleation events at the solid/liquid interface of the pro-peritectic phase. These nucleation events led to isothermal peritectic growth. Thus, the experimental investigations confirmed the theoretically predicted morphology at least qualitatively.
- After the nucleation events, the peritectic phase grew lamellar in a zig-zag pattern at first. The proportion of peritectic phase did not remain constant, but decreased. This reduction changed the growth from lamellar to fibrous. The temperature level of the solid/liquid interface dropped constantly to lower temperatures during the coupled growth. When the interface fell below the temperature range of 401 ± 2 K, the peritectic phase completely disappeared and the coupled growth turned into a planar growth of the pro-peritectic phase.
- The nucleation event of the peritectic phase occurred in the case where the planar solid/liquid interface of the primary phase shows small perturbations, otherwise not. It looks like the necessary surface roughness of the pro-peritectic phase was not present at lower pulling velocities.
- During the coupled growth, the solid/liquid interface does not grow at the invariant peritectic temperature, or with constant undercooling but decreases to lower and lower temperature levels. Apart from speculative assumptions, this finding could not be explained with the available experimental data, and therefore, further investigations are needed.

Acknowledgements This work was supported in part by the European Space Agency ESA and in part by the Austrian Space Agency ASA through means of the ESA MAP project METCOMP (AO-1999-114), the hardware was developed by QinetiQ Space, and the μg-experiment operations were carried out by the team at E-USOC.

References

1. Park JS, Trivedi R (1998) Convection-induced novel oscillating microstructure formation in peritectic systems. J Cryst Growth 511–515
2. Yasuda H, Ohnaka I, Tokieda K (1997) In-situ observation of peritectic solidification in Sn-Cd and Fe-C alloys, Solidification processing, University of Sheffield, pp 44–48
3. Boettinger WJ (1974) The structure of directionally solidified two-phase Sn-Cd peritectic alloys. Metall Trans 5:2023–2031
4. Su YQ, Luo LS, Li XZ, Guo JJ, Yang HM, Fu HZ (2006) Well-aligned in situ composites in directionally solidified Fe-Ni peritectic system. Appl Phys Lett 89:2319181–2319183

5. Luo LS, Su YQ, Guo JJ, Li HZ, Yang HM, Fu HZ (2008) Producing well aligned in situ composites in peritectic systems by directional solidification. Appl Phys Lett 92:0619031–0619033
6. Dobler S, Lo TS, Plapp M, Karma A, Kurz W (2004) Peritectic coupled growth. Acta Mater 52:2795–2808
7. Trivedi R (1995) Theory of layered structure formation in peritectic system. Metall Mater Trans 26A:583–590
8. Hunziker O, Vandyoussefi M, Kurz W (1998) Phase and microstructure selection in peritectic alloys close to the limit of constitutional undercooling. Acta Mater 46:6325–6336
9. Lo TS, Karma A, Plapp M (2001) Phase-field modeling of microstructural pattern formation during directional solidification of peritectic alloys without morphological instability. Phys Rev E 63:031504
10. Trivedi R (2005) The role of heterogeneous nucleation on microstructure evolution in peritectic systems. Scripta Mat 53:47–52
11. Barrio M, Lopez DO, Tamarit JL, Negrier P, Haget Y (1995) Degree of miscibility between non-isomorphous plastic phases: binary system NPG (Neopentyl-glycol)-TRIS tris(hydroxymethyl)aminomethane. J Mater Chem 5(3):431–439
12. Ludwig A, Mogeritsch JP, Grasser M (2009) In situ observation of unsteady peritectic growth modes. Trans Indian Inst Met 62:433–6
13. Mogeritsch JP, Eck S, Grasser M, Ludwig A (2010) In situ observation of solidification in an organic peritectic alloy system. Mater Sci Forum 649:159–164
14. Ludwig A, Mogeritsch JP (2011) In situ observation of coupled peritectic growth. In: John Hunt international symposium london, pp 233–242
15. Mogeritsch JP, Ludwig A, Pfeifer T (2017) In-situ observation of coupled peritectic growth in a binary organic model alloy. Acta Mater 126:329–335
16. https://www.qinetiq.com/en/sectors/space
17. http://www.sigmaaldrich.com. Accessed 23 Aug 2021
18. NPG CAS-No 126–30–7 and TRIS CAS-No 77–86–1
19. Kurz W, Fischer DJ (1998) Fundamentals of solidification. Trans Tech Publications Ltd. ISBN 0–87849–804–4

523312_1_En_136_Chapter ☑ TYPESET ☐ DISK ☐ LE ☑ CP Disp.:30/11/2021 Pages: 13 Layout: T1-Standard

MARKED PROOF

Please correct and return this set

Please use the proof correction marks shown below for all alterations and corrections. If you wish to return your proof by fax you should ensure that all amendments are written clearly in dark ink and are made well within the page margins.

Instruction to printer	*Textual mark*	*Marginal mark*
Leave unchanged	··· under matter to remain	New matter followed by
Insert in text the matter indicated in the margin		or (x2)
Delete	through single character, rule or underline or through all characters to be deleted	or (x2)
Substitute character or substitute part of one or more word(s)	through letter or through characters	new character or new characters
Change to italics	under matter to be changed	
Change to capitals	under matter to be changed	
Change to small capitals	under matter to be changed	
Change to bold type	under matter to be changed	
Change to bold italic	under matter to be changed	
Change to lower case	Encircle matter to be changed	
Change italic to upright type	(As above)	
Change bold to non-bold type	(As above)	
Insert 'superior' character	through character or where required	or under character e.g. or
Insert 'inferior' character	(As above)	over character e.g.
Insert full stop	(As above)	
Insert comma	(As above)	
Insert single quotation marks	(As above)	or and/or or
Insert double quotation marks	(As above)	or and/or or
Insert hyphen	(As above)	
Start new paragraph		
No new paragraph		
Transpose		
Close up	linking characters	
Insert or substitute space between characters or words	through character or where required	
Reduce space between characters or words	between characters or words affected	